

crystals obtained with slow cooling: non-centrosymmetric I41cd and I41/acd with centrosymmetry. The I41cd and I41/acd symmetry difference is a reflection of the varied ordering type of CdAs_4 tetrahedral units packed in a large unit cell of stacked fluorite-like structure with vacancies. The Cd_3As_2 crystal structure studied in this work can be satisfactorily indexed with space group I41cd.

The band structure of the grown Cd_3As_2 single crystal was characterized with ARPES measurements at beam line 4.0.3 at Advanced Light Source in Berkeley, California. Sharp XPS signals at binding energies $\text{EB} \sim 11$ and 41 eV that correspond to cadmium 4d and arsenic 3d core levels were observed, confirming the chemical composition of the Cd_3As_2 single crystal to be correct. Remarkably, a low-lying small feature that crossed the Fermi level was observed, which corresponds to surface bands of Cd_3As_2 . The linearly dispersive upper Dirac cone is notably located at the surface Brillouin zone center; the Dirac point is found at binding energy 200 meV. The spectral characterization shows a linear dispersive band, thus confirming the high quality of the sample. The surface structure of the vacuum-cleaved Cd_3As_2 surface was further explored with STM measurements. The observed pseudo-hexagonal nearest-neighbor lattice spacing 0.435 nm is near that expected for the (112) surface. Tunneling spectra were subsequently recorded for this (112) surface. The results reveal a conductance minimum at approximately 200 meV below the Fermi level, consistent with the energy of the Dirac point observed in the ARPES data. The approximately linear increase in conductance above this point is consistent also with the linearly dispersive upper Dirac cone observed using ARPES. Resistivity data were measured using a standard four-probe method. The temperature dependence of the resistivity shows that metallic behavior is observed in Cd_3As_2 crystals. The resistivity is nearly independent of temperature below $T = 5$ K, giving a residual resistivity in the range approximately $0.2\text{--}0.4$ m Ω cm. The Hall resistivity is practically linear under a magnetic field up to 15 T with the Shubnikov-de Haas oscillation appearing at higher fields.

Their work delivers large plate-like high-quality single crystals of Cd_3As_2 with large facets of (112) and (even 00) planes prepared with a self-selecting vapor growth method. The combination of ARPES, STM and transport measurements revealed the unique band structure of 3D Dirac semimetal Cd_3As_2 . (Reported by Ying-Hao Chu)

This report features the work of Fang-Cheng Chou and his co-workers published in Sci. Rep. 5, 12966 (2015).

Reference

1. R. Sankar, M. Neupane, S.-Y. Xu, C. J. Butler, I. Zeljkovic, I. P. Muthuselvan, F.-T. Huang, S.-T. Guo, Sunil K. Karna, M.-W. Chu, W. L. Lee, M.-T. Lin, R. Jayavel, V. Madhavan, M. Z. Hasan, and F. C. Chou, *Sci. Rep.* **5**, 12966 (2015).

Interlayer Coupling Affects the Growth of 2D Stripe Orders

Doped Mott insulators have served as a rich playground for strongly correlated electron systems, but the physics is incompletely comprehended. The complication results from an interplay between competing orders, such as charge, spin, orbital and lattice, and strong quantum fluctuations.¹ In high- T_C superconductor $\text{La}_{2-x}\text{Sr}_x\text{CuO}_4$ (LSCO), in which holes are doped into the antiferromagnetic (AFM) Mott insulating La_2CuO_4 , unidirectional self-organized electronic stripes are induced in plane $a \times b$ of the crystal space.² This intralayer coupling between the ordered charges and spins has been widely discussed; it is natural to ask what role the interlayer coupling between the charge and spin orders in separate planes plays in these systems.

$\text{La}_{2-x}\text{Sr}_x\text{NiO}_4$ (LSNO) has a tetragonal structure, shown in Fig. 1(a), and is isostructural with the superconducting cuprate LSCO. Both LSCO and LSNO are AFM Mott insulators in the absence of hole doping. While LSCO becomes a high- T_C superconductor with hole doping to a small extent, LSNO remains insulating for doping levels up to 90%.³ LSNO, however, shows an alternating pattern of AFM domains (spin stripes) separated by charge stripes within each two-dimensional NiO layer, shown in Fig. 1(b);⁴ the stripes lead to charge and spin satellite reflections with wave vectors $Q_{\text{CO}} = (H \pm 2\epsilon, 0, L_1)$ and $Q_{\text{SO}} = (H \pm \epsilon, 0, L_2)$, in which H and L_2 are integers, L_1 is odd and ϵ is determined by the hole concentration with $\epsilon \sim x$. For

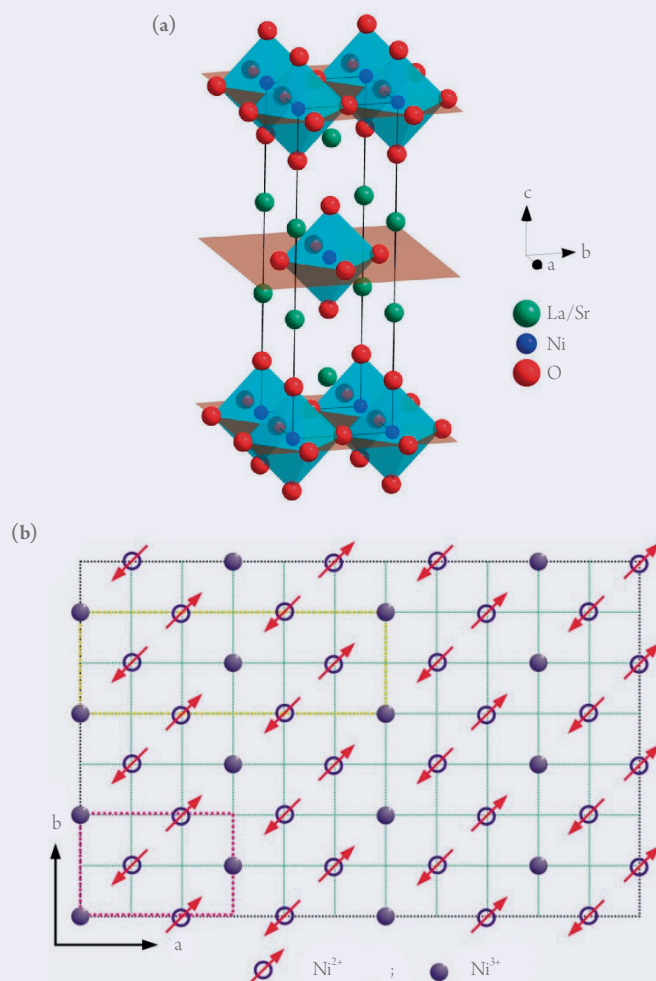


Fig. 1: (a) Crystal structure of LSNO. (b) Schematic view of charge and spin stripes in LSNO in NiO_2 planes. The arrows represent Ni^{2+} ions and solid circles are the holes. Yellow and red boxes indicate the size of spin and charge modulations. [Reproduced from Ref. 5]

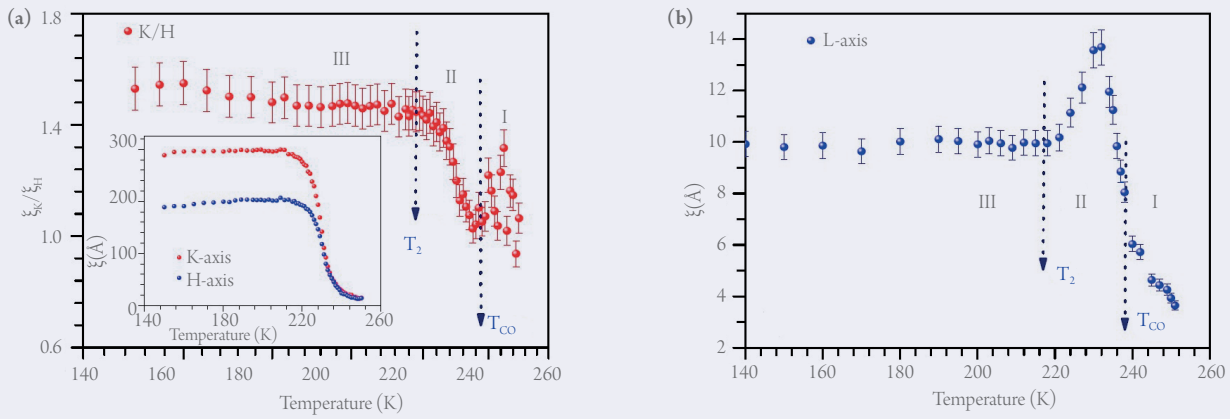


Fig. 2: (a) Temperature dependence of the ratio of correlation lengths of the charge stripe along directions H and K . The inset shows the temperature dependence of each correlation length. (b) Temperature dependence of the correlation length of the charge stripe along direction L . [Reproduced from Ref. 5]

$\text{La}_{1.67}\text{Sr}_{0.33}\text{NiO}_4$ ($x = 1/3$), the charge and spin orders are commensurate with the lattice as ϵ is $1/3$.

Studying charge and spin ordering of stripes in $\text{La}_{1.67}\text{Sr}_{0.33}\text{NiO}_4$ measuring X-ray scattering, Shu-Han Lee, Chao-Hung Du and their co-workers⁵ reported an atypical inverse order-disorder transition of charge stripes due to interlayer coupling of the in-plane charges and spins. They measured X-ray scattering of charge-ordering reflection of LSNO at **BL07A1** and **SP12B1**; the incident photon energy was selected to be 10 keV. For spin-stripe reflection, they measured also resonant soft X-ray scattering at the Ni L_3 edge at **BL05B3**.

Figure 2(a) shows the temperature dependence of the ratio of correlation

lengths of the charge stripe along directions H and K in reciprocal space. On the basis of the temperature dependence, they divided the charge-ordered phase into three regions with two transition temperatures, T_{CO} (~ 238 K) and T_2 (~ 218 K). In regime I ($T > T_{CO}$), the segregated charges are in a disordered and isotropic state. Upon cooling, the segregated charges form anisotropic charge stripes; the anisotropy displays a temperature-dependent behaviour in regime II ($T_2 < T < T_{CO}$). The anisotropy becomes eventually nearly constant in regime III (below T_2).

The atypical inverse order-disorder transition is observed in measurements of the correlation lengths of charge ordering taken along direction L in reciprocal space, as shown in Fig. 2(b). Cooling from high temperatures, the

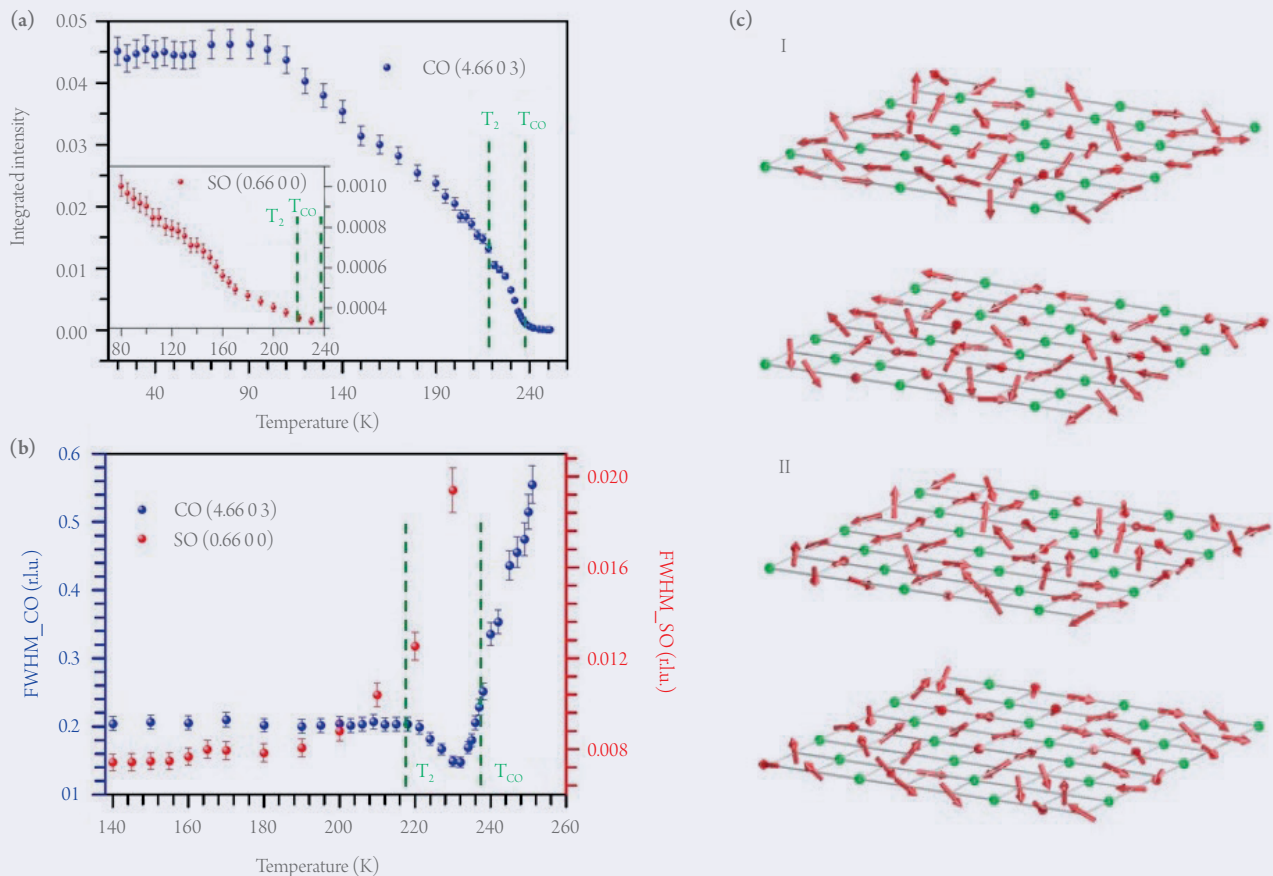


Fig. 3: Temperature dependence of (a) integrated intensity and (b) line width for CO reflection (4.66, 0, 3) (blue dots) and SO reflection (0.66, 0, 0) (red dots). (c) Real-space configurations of the states in regimes I and II. [Reproduced from Ref. 5]

charge correlation begins to build significantly along axis c of the crystal at T_{CO} ; the charge correlation length begins to increase from $\xi = \sim 6 \text{ \AA}$ to 14 \AA as temperature decreases to 230 K. At 230 K, the interlayer charge correlation spans over two NiO layers; it seems that a full 3D ordering would eventually develop, but on further decreased temperature the interlayer charge correlation begins to decrease and an inverse order-disorder transition occurs. The interlayer charge correlation length eventually attains $\xi = \sim 10 \text{ \AA}$ below $T_2 = 218 \text{ K}$, at which both the charge and spin stripes are established.

To consider the origin of the inverse order-disorder transition in the interlayer charge correlation, they compared the temperature dependence of the charge-ordering (CO) reflection (4.66, 0, 3) and the spin-ordering (SO) reflection (0.66, 0, 0). Figure 3(a) compares the temperature dependence of the integrated intensity of the CO and SO reflections. The weak spin-ordering reflection is, notably, still observable at temperature 230 K, which indicates a strong coupling between the charge and spin stripes.

They compared also temperature dependence of the line width of a SO reflection (0.66, 0, 0) measured along direction H and that of a CO reflection (4.66, 0, 3) along direction L in Fig. 3(b). The former serves as a measure of in-plane spin order and the latter as a measure of interlayer charge correlation. Although the spin-stripe transition occurs at $\sim 190 \text{ K}$, the satellite SO reflection persists to a temperature as high as 230 K, indicating a dynamic spin fluctuation at high temperatures. The onset of the interlayer charge-order suppression at 230 K coincides with the appearance of the in-plane spin-stripe order, which indicates that the in-plane spin-stripe order plays an important role in the inverse transition of the interlayer charge order.

Lee *et al.* intuitively explained the curious rise and fall of the interlayer correlation as a result of two competing interactions. The interlayer charge-charge coupling favors the stripes in separate layers to be out of phase because the charge stripes repel each other, whereas the interlayer charge-spin coupling

favors in-phase stripes because the formation of in-plane spin modulation causes a dissipation of the kinetic energy of the electrons. In-plane charge order appears first, resulting in the building of an out-of-phase interlayer charge correlation, but, as the in-plane spin-stripe order begins to develop, the interlayer charge order is suppressed. Figure 3(c) indicates the real-space configurations for regimes I and II: in regime I, there exists no or weak in-plane charge order and correlation between layers is small; in regime II, the charge-stripe order develops whereas the spins remain disordered. Out-of-plane charge correlation develops to minimize the Coulomb repulsion. In regime III, spin order develops and the out-of-plane charge correlation is suppressed; the system transforms into a three-layer stacking.

Their work points to the importance of the interlayer coupling in LSNO. An interlayer Coulomb interaction has been argued to be crucial to understand an anomalous shrinking of ratio c/a of lattice parameters that correlates with T_{CO} in LSNO, as well as the existence of fluctuating charge stripes that persist to high temperatures. In particular, the inverse order-disorder transition of the interlayer charge order observed in their work might provide a new direction to understand the dominance of the dynamical stripes in cuprates. (Reported by Jun Okamoto)

This report features the work of Shu-Han Lee, Chao-Hung Du and their co-workers published in Phys. Rev. B 92, 205114 (2015).

References

1. P. A. Lee, N. Nagaosa, and X.-G. Wen, *Rev. Mod. Phys.* **78**, 17 (2006).
2. J. M. Tranquada, B. J. Sternlieb, J. D. Axe, Y. Nakamura, and S. Uchida, *Nature* **375**, 561 (1995).
3. R. J. Cava, B. Batlogg, T. T. Palstra, J. J. Krajewski, W. F. Peck, A. P. Ramirez, and L. W. Rupp, *Phys. Rev. B* **43**, 1229 (1991).
4. S. H. Lee, J. M. Tranquada, K. Yamada, D. J. Buttrey, Q. Li, and S.-W. Cheong, *Phys. Rev. Lett.* **88**, 126401 (2002).
5. S.-H. Lee, Y.-C. Lai, C.-H. Du, A. F. Siegenfeld, Y.-J. Kao, P. D. Hatton, D. Prabhakaran, Y. Su, and D.-J. Huang, *Phys. Rev. B* **92**, 205114 (2015).

